

We are IntechOpen, the world's leading publisher of Open Access books Built by scientists, for scientists

6,900

Open access books available

186,000

International authors and editors

200M

Downloads

Our authors are among the

154

Countries delivered to

TOP 1%

most cited scientists

12.2%

Contributors from top 500 universities



WEB OF SCIENCE™

Selection of our books indexed in the Book Citation Index
in Web of Science™ Core Collection (BKCI)

Interested in publishing with us?
Contact book.department@intechopen.com

Numbers displayed above are based on latest data collected.
For more information visit www.intechopen.com



Composite Material and Optical Fibres

Antonio C. de Oliveira and Ligia S. de Oliveira

Additional information is available at the end of the chapter

<http://dx.doi.org/10.5772/76664>

1. Introduction

For ease of handling and polishing, optical fibres are generally mounted in some form of rigid structure. A schematic of a typical fibre termination used in astronomical instruments (typical of multiple-fibre spectrographs) is shown in Fig. 1. The fibre is first placed within a flexible tube (polyimide or similar), often referred to as the strain relief tube. The fibre and tube are placed within a rigid ferrule. Adhesive is applied to the fibre and tubing to fix them in place. The ferrule can then be easily manipulated for polishing, or mounting within an instrument, without risk of damage to the fibre. The role of the strain relief tube is to prevent stresses occurring at the point where the fibre enters the ferrule given bending at this point may lead to breakages. For coupling an array of optical fibres to a microlens array, such as in IFU (Integral Field Unity), a brass plate with an array of drilled microholes may be used. Optical fibres positioned in an array of accurately drilled holes, as illustrated schematically in Fig. 2.

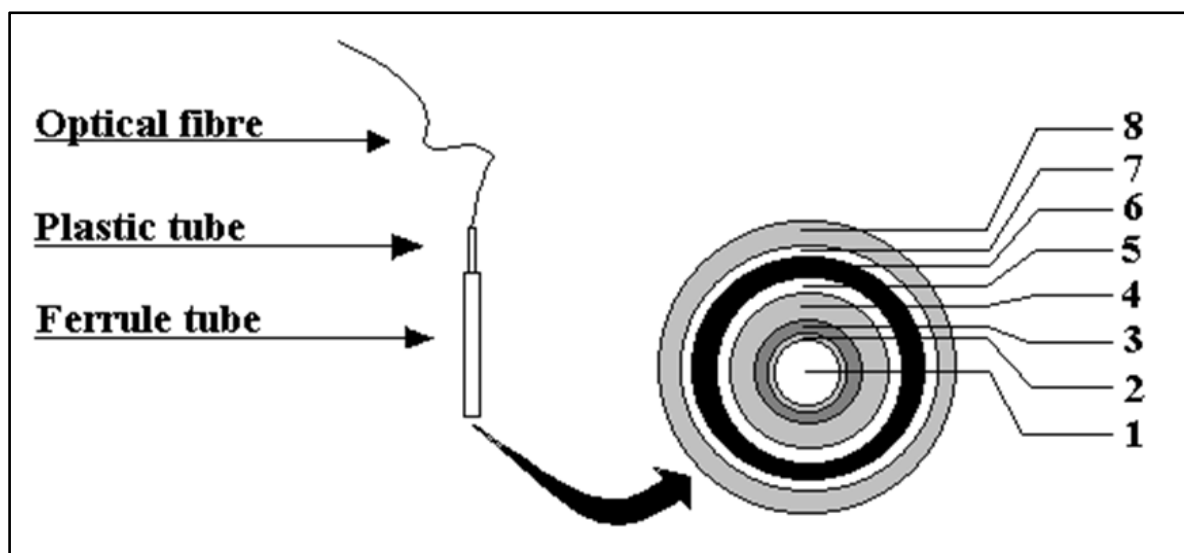


Figure 1. Schematic diagram of a single fibre mounting assembly: 1, core; 2, cladding; 3, polyamide buffer; 4, acrylate buffer; 5, epoxy; 6, plastic tube; 7, epoxy; 8, ferrule steel tube.

This system, called microholes array, contains a grid of holes spaced by the pitch of the microlens array. The holes are machined using custom made drills with two different diameters. This produces a stepped hole, with the smaller diameter hole used for fibre positioning while the larger hole is used to accommodate a ferrule. The small holes are approximately 10 μm larger than the fibre diameter to allow sufficient space for a glue to penetrate. Using a stepped hole also allows a greater depth of material to be machined than by using a small drill alone. This permits a thicker, hence more robust, piece of material to be used. A support plate is also used, positioned above the fibre-positioning array with spacers, to maintain accurate angular alignment of the ferrules with respect to the microlens optical axis. Each ferrule contains a polyimide strain relief tube to prevent mechanical stress, occurring at the point where the fibre enters the ferrule. To secure the fibres, ferrules, and polyamide tubes in place the whole input assembly is immersed in a container of EPOTEK 301-2 adhesive. This epoxy is a natural choice due to its excellent wicking properties and low shrinkage upon curing. After curing, which takes approximately three days at room temperature; any excess glue is removed prior to optical polishing.

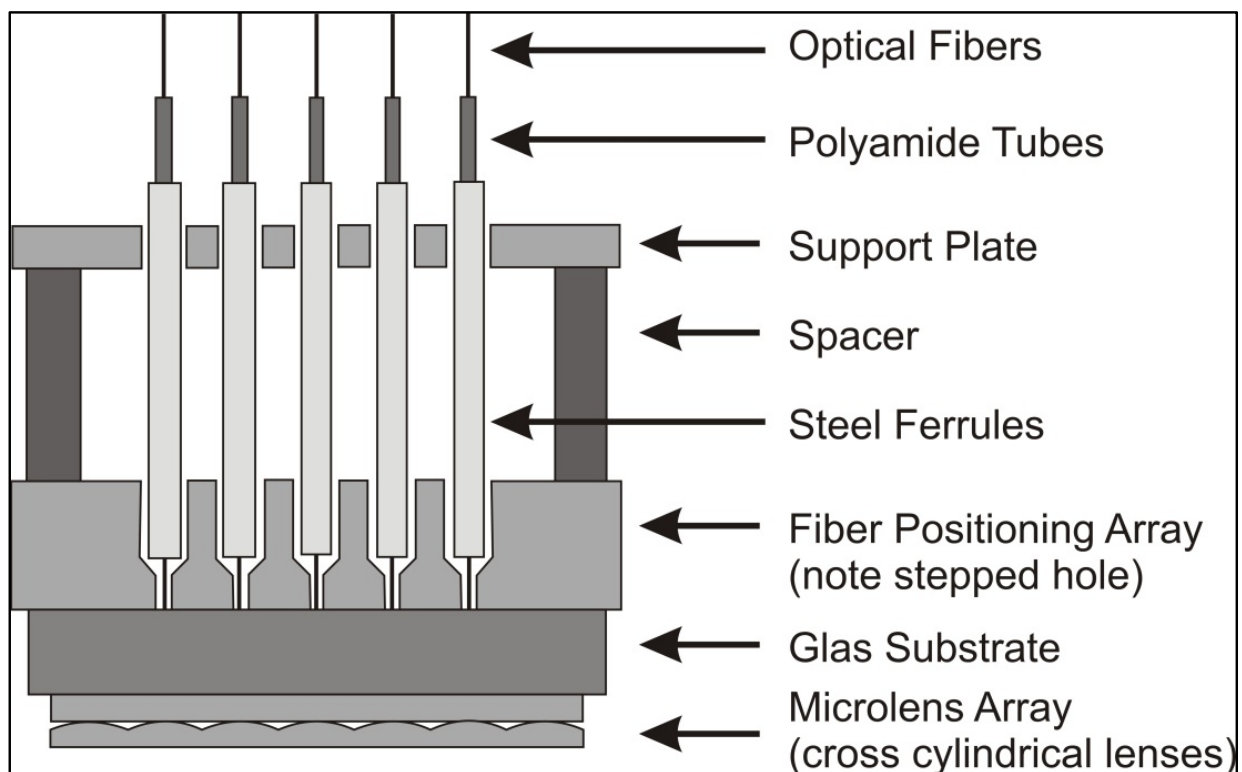


Figure 2. Schematic micro lens array and fibre positioning array used to constructed IFUs

The problem here may be an increase of FRD (Focal Ratio Degradation) caused by contraction of the metal ferrule or brass plate at low temperature causing stress on the fibres and consequent loss of throughput. Astronomic instruments like that in general work in environments with significant thermal gradients, a common characteristic of ground-based observatories. An interesting alternative to the conventional steel ferrule may be a quartz tube. Quartz material has no problems of contraction in the temperature gradients experienced in that places, $-10\text{ }^{\circ}\text{C}$ to $20\text{ }^{\circ}\text{C}$, but is very expensive and difficult to obtain. The

ideal condition requires a material with elasticity controlled so as not to cause stress or shift the positioning of optical fibre under temperature gradients. For just such purposes, we have developed a special composite formed from a mixture of EPO-TEK 301-2 and some refractory material oxide in nano-particle form, cured and submitted to a customized thermal treatment. To avoid bubbles and points of stress, this mixture is prepared in a separate receptacle inside a vacuum chamber. The resulting material is more resistant and harder than EPO-TEK 301-2 and is found to be well suited to the fabrication of optical fibre arrays. An important secondary characteristic is the ease with which it can be polished. This feature is a result of the micro particles, which keep the polished surface very homogeneous during the final polishing procedure. The resulting composite combines the beneficial characteristics of both the epoxy and the oxide; main factor its coefficient of thermal expansion is significantly lower than simple solidified epoxy; the exact value depending on the relative concentrations. While the characteristics of this particular composite are still under study, it is clearly possible to deploy this material in the construction of devices for several fibre instruments.

2. New materials to support optical fibres

Similar microholes arrays and the support plates of the Fig. 2, used to construct Eucalyptus IFU, were made with toolmakers brass (de Oliveira et al., 2002). The problem here is that differential expansion between the metal array and the glass microlens substrate may lead to the bond between them failing at low temperatures. Although the coefficient of thermal expansion of epoxy is much greater than those of steel, brass or glass, the elasticity of the epoxy accommodates the dimensional changes without breakage: however, this can introduce a small amount of stress build-up.

It is well known that mechanical deformation causes focal ratio degradation (FRD) by the formation of microbends in the fibre (Clayton 1989). FRD is a non-conservation of *étendue* such that the focal ratio is broadened by propagation in the fibre. When mounting the fibre, the appropriate epoxy and tubing should be selected, and general care must be taken to minimize mechanical stress and avoid additional FRD (de Oliveira et al., 2005). This is straightforward at room temperature, but greater care must be taken in the choice of materials for use at low temperatures. When the fibre assembly is cooled to temperatures around $-10\text{ }^{\circ}\text{C}$, the epoxy, tubing and ferrule will all shrink differentially, and this may cause the level of FRD to increase. There is other problem when the fibre assembly is warmed to around $20\text{ }^{\circ}\text{C}$ and cooled to around $-10\text{ }^{\circ}\text{C}$. The UV epoxy, currently used to cement the metal and the glass may be damaged if the system will be submitted several times at big changes of temperature. In this case the system may detach in places due the thermal gradient.

Microholes array and support plate made with solidified EPOTEK represent a first step to change the metallic base for a polymeric base. The choice of the EPOTEK 301-2 is appropriate due to its excellent wicking properties and low shrinkage upon curing. This properties are very good to use in optical fibres system, so that, if it is possible to get plates

adequate to machine with this epoxy we can get total compatible in the construction of the system.

2.1. Epoxy solidified

The epoxy EPO-TEK 301-2 has low viscosity and requires a container to constrain its flow until it is solidified. Generally aluminium has been used to make these containers but it is possible to use brass, plastic or acrylic. The complete curing process takes approximately three days at room temperature and when it is dry, it is transparent to visible light. To avoid bubbles and points of stress, the epoxy is prepared in a separate container inside a vacuum chamber. The correct amount is allowed to set in the container, which is placed inside a dry environment. Once cured, some thermal treatment may be necessary. Several kinds of blocks, cylinders and plates can be made to test the polishing qualities of these test pieces. The results are very encouraging with the hardness similar to acrylic resin. The Fig. 3 and 4 shows steps to obtain samples machined to manufacture blocks of epoxy solidified.

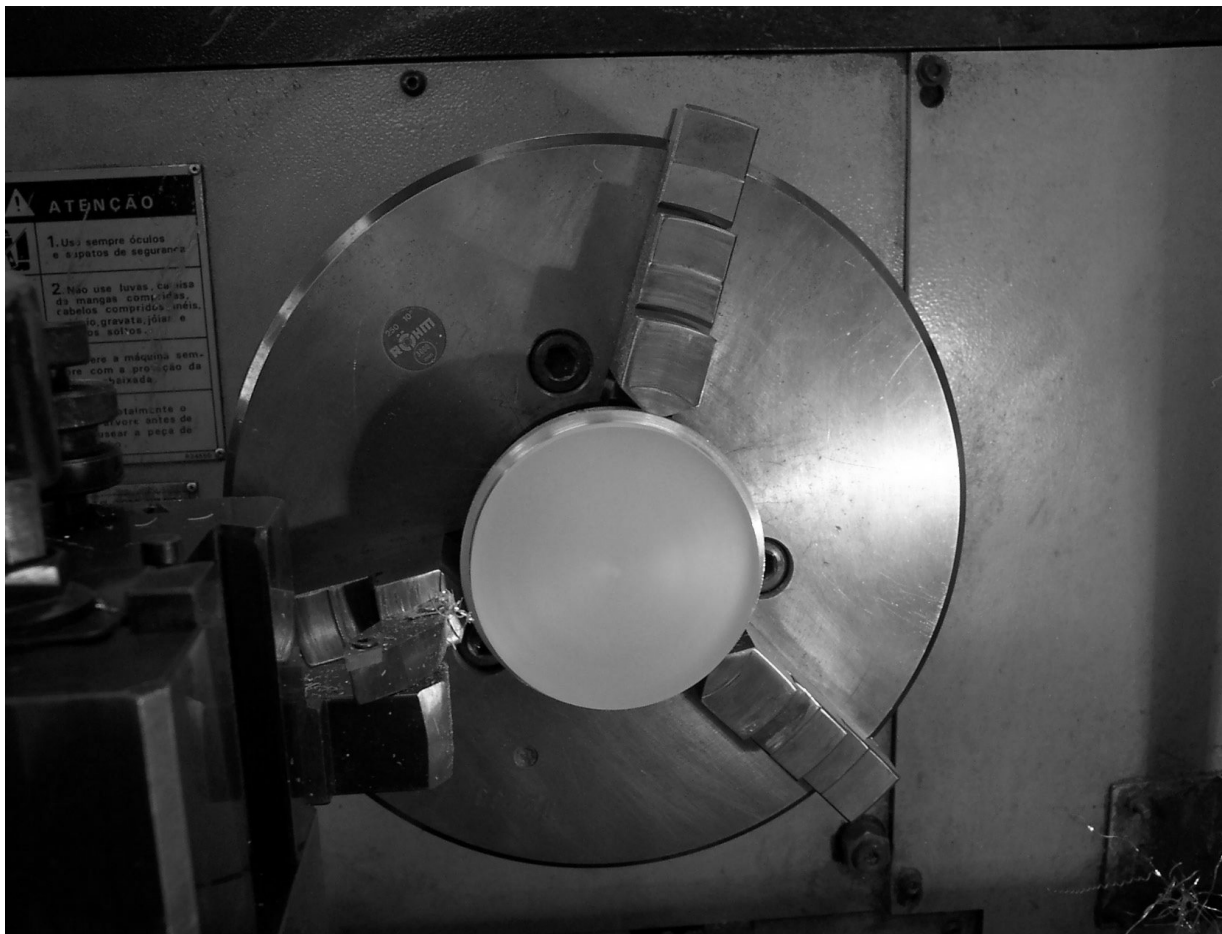


Figure 3. EPO-TEK 301-2 solidified, during the machining procedure

Machining quality is important as burrs inside the microholes may prevent the fibres from being threaded into the holes, or cause stress, or breakage, of the fibres. The quality of such microhole arrays inspected visually using a microscope, give very encouraging results

displaying a minimum of burring; scarf, remaining in the holes, may be readily removed by cleaning in an ultrasonic bath.

There are several advantages to the use of solidified epoxy as compared to brass, for example, in the fabrication and use of fibre support devices. Ease of machining and compatibility with other epoxies used to attach glass or silica, may be the most important of these advantages. Although the coefficient of thermal expansion of epoxy is much greater than that of steel or glass, Tab. 1, its elasticity accommodate thermally induced dimensional changes without breakage. This also avoids excessive stress associated with increases in FRD but, in principle, could be deleterious in compromising the critical positioning stability of optical fibres as the temperature varies.

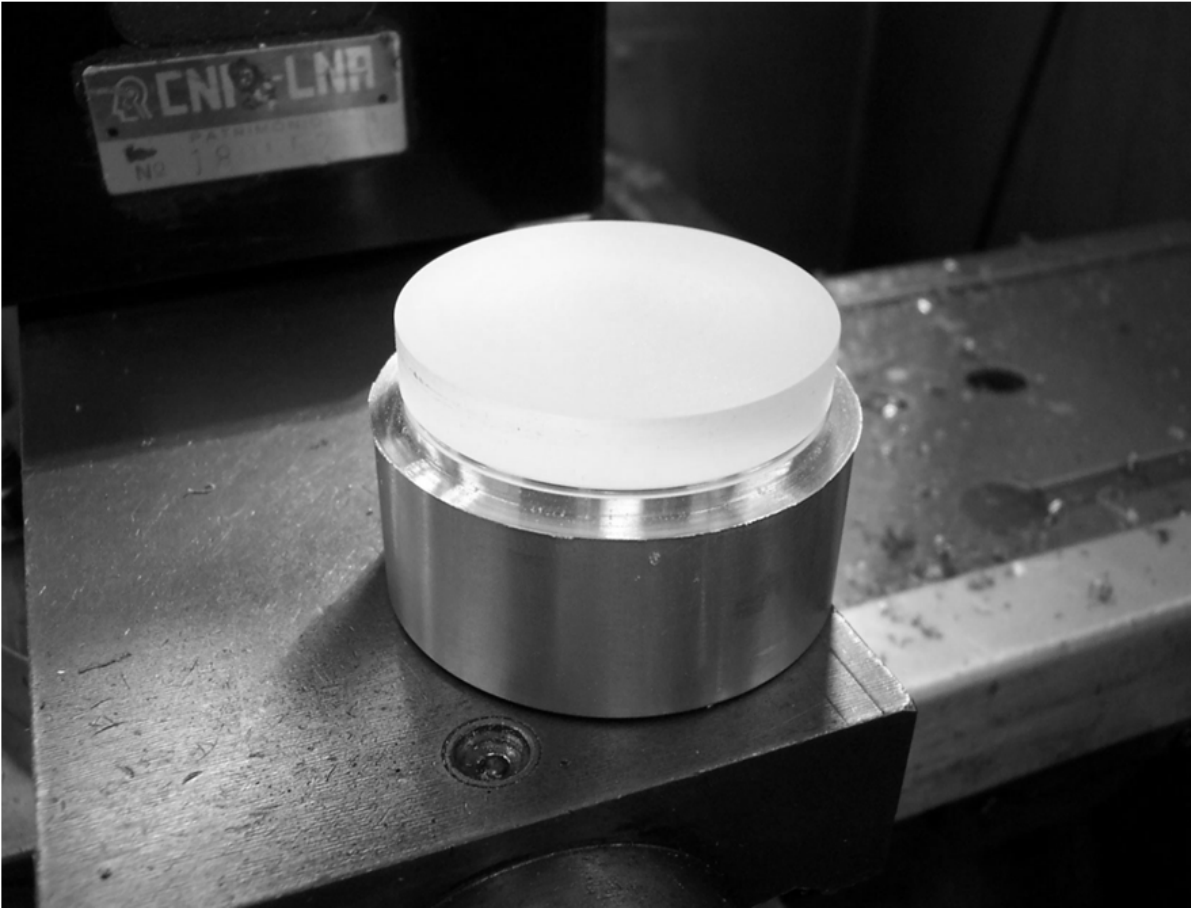


Figure 4. Plate of EPO-TEK 301-2 solidified and machined

Material	α CTE at 20 °C	Units
Brass	19	$10^{-6} / ^\circ\text{C}$
Carbon Steel	10.8	$10^{-6} / ^\circ\text{C}$
In ox Steel	17.3	$10^{-6} / ^\circ\text{C}$
Quartz	0.59	$10^{-6} / ^\circ\text{C}$
EPO-TEK 301-2	55 at 61	$10^{-6} / ^\circ\text{C}$

Table 1. Coefficient of Thermal Expansion of some materials

Machining quality is important as burrs inside the microholes could prevent the fibres from entering the hole, cause stress, or breakage, of the optical fibres. The quality of the microholes array may be inspected visually using a binocular microscope and the results are often very satisfactory with minimal burring present. Swarf present in the holes is readily removed by cleaning in an ultrasonic bath. The Fig. 5 shows a sample of epoxy solidified with a microholes array.

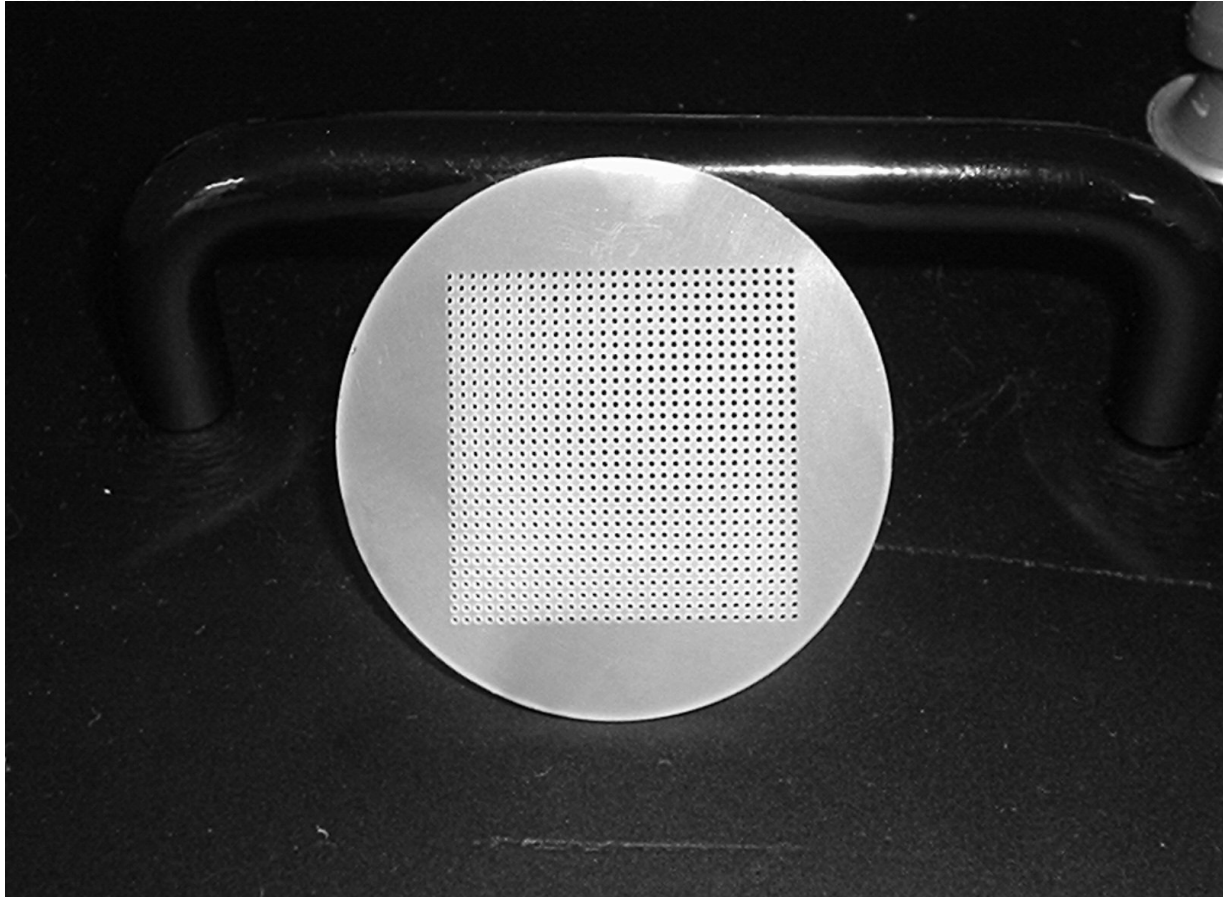


Figure 5. Photograph of the microholes array in a sample of the EPO-TEK 301-2 solidified

After machined, this sample has a diameter of 48 mm and a thickness of 3 mm. This microholes array is matrix 30x30 holes spaced on a 1.0 mm pitch. The holes were machined using custom made drills with diameters of 0.60 mm and 0.21 mm. This produces a stepped hole, with the smaller diameter hole used for fibre positioning while the larger hole is used to accommodate a ferrule. The small holes are approximately 10 μm larger than the fibre diameter to allow sufficient space for glue penetrates. The machining error in the position of the small holes was measured to be approximately 2 μm .

2.2. Experimental stress analyses

It is possible to use a very simple experiment of Photo elasticity method to evaluate the static stress in the plates of epoxy solidified. Classical two-dimensional photo elasticity is an optical experimental technique for determining stress fields in solids bodies. For a given

analysis, polarized light is passed through a transparent sample or the body in question, and stress-induced or static stress changes in the light result in an interference-like pattern, which may be analysed to determine the principal stresses at each point within the body.

The basis for photo elastic measurement is a phenomenon of double refraction (also called artificial birefringence). There are two situations that may cause this phenomenon. Certain plastics exhibit the first situation when the sample of this type is subjected to an applied load, the resulting stress /strain field causes the molecules within the transparent material to have a preferred alignment. The second situation is exhibited by certain epoxies after dried and in this case the stress may be called static stress. In both situations the light wave vibrations have two preferred directions within the material and a wave of linearly polarised light entering the field is split into two waves which are linearly polarised at right angles to each other and which propagate with different velocities. That is, two rays travel along each an original line of propagation, and their electric vectors are mutually perpendicular. In fact, each vibration is collinear with one of the principal stress directions. (See Fig. 6.) Also, since the two waves travel at different velocities, a phase difference develops between them and by using certain optical elements.

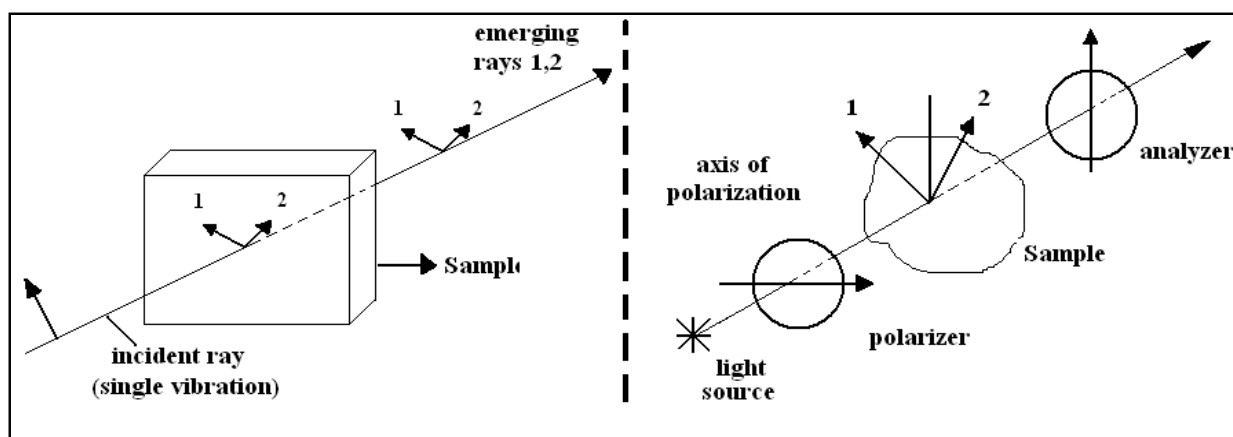


Figure 6. Left: propagation of light through photo elastic models. Right: plane polariscope used to get information of the stress inside of the sample by analyse of the artificial birefringence.

A very simple system to get qualitative images of the samples may be adapted with a transmission Polariscope, as shown in Fig. 6. The system uses a CCD camera to take the images. Stresses within solidified EPO-TEK 301-2 may be investigated with the use of the photo elasticity method whereby stress-induced birefringence is measured using polarized light. Static stress can be recorded as an interference pattern, which may be analysed to determine the principal stresses at each point within the material. Indeed, significant stress induced birefringence is detected in such samples, as is shown in Fig.7 side left.

This stress can be alleviated through thermal shock induced by warming the sample to 80 °C for 30 min. Fig. 7 side right demonstrates the reduction in stress as the material is returned to room temperature. Of course, such experiments are only viable for transparent materials but they do give a warning that care must be taken in analysing the effects of thermally induced stress through measurement of fibre displacement in arrangements and FRD stress-induced.



Figure 7. Left: sample before thermal shock. Right: same sample after thermal shock

2.3. Composite

It is possible to create composites using a mix of epoxy and several types of oxides in micro or nano-particle form. To avoid stress points and heterogeneous regions, the composite needs to be prepared using mixers of high speed. Ultrasonic chamber can be useful to ensure more uniformity to the mixture. Before the cure, this composite requires to be subjected to a vacuum of 10^{-3} Torr to reduce bubbles inside of material. The mixture of EPO-TEK 301-2 with refractory material oxide in nano-powder, cured and submitted to a thermal treatment around $400\text{ }^{\circ}\text{C}$, produce a very interesting option instead simple epoxy solidified. The resulting material is more resistant and harder than EPO-TEK 301-2 and is found to be well suited to the fabrication of optical fibre arrays. Several different refractory material oxides in nano-powder may be used to produce different characteristics in this type of composite. So it is possible to combine Zirconium oxide, Barium oxide, Silica oxide, Cerium oxide and others, Fig. 8, to obtain a material optimized to specific applications. The solidified mixture combines the beneficial characteristics of both the epoxy and the oxide; main factor its coefficient of thermal expansion is significantly lower than simple solidified epoxy; the exact value depending on the relative concentrations.

There are two important factors that consolidate the structure of this composite. The first is the process of cure of the liquid mixture. The second is the process of heating of the solid material obtained after the cure. The chemical reactions during the first process are limited by the time to reach the complete cure of the epoxy. Anyway, chemical analysis showed no evidence of endothermic or exothermic chemical reactions between oxides and epoxy. In fact, the materials involved in the mixture appear quite neutral. However, the heating procedure in temperatures around $400\text{ }^{\circ}\text{C}$ with slow cooling during 24 hours induces slight shrinkage on the material. Although the study still lacks depth, it is fairly simple to conclude that the structure undergoes some type of molecular rearrangement with some material loss and subsequent compaction. In fact this process carbonizes the external side of the solid material. To avoid total and destructive carbonization, both, the heating and cooling is done with the composite inside a steel container with refractory sand. After this procedure, the external part carbonized can be removed by machining process leaving the sample completely clean. The material thus obtained proves to be quite stable and resistant even

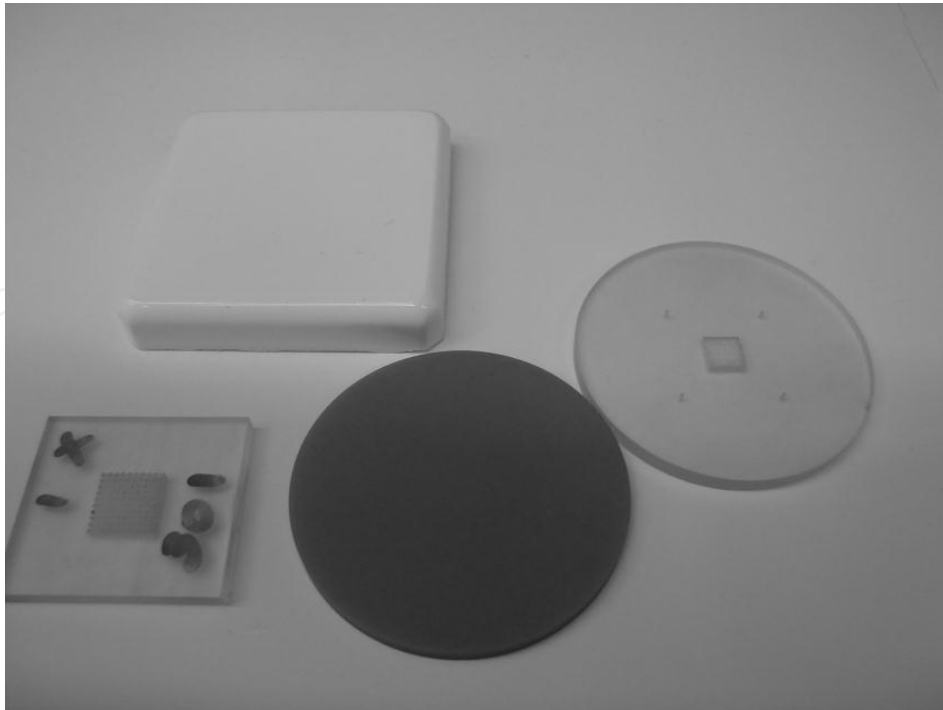


Figure 8. Samples of different composites at the centre and epoxy solidified at the borders

though it has some degree of slow oxidation on its surface. This oxidation is evident from the slight colour change after a few weeks of exposure and manipulation, but still remains a high physical stability.

This composite has two physical characteristics very interesting for the construction of optical fibres holders. The first feature is its ability to sustain their polishing, with minimum quantities of abrasives during this procedure. In other words, when the composite is subjected to a polishing of high performance, the detachment of the refractory oxide nanoparticles reinforces gently the polishing process and increasing the efficiency of this procedure. The surface roughness measured in several samples, after high performance polishing was about 0.01 microns. Furthermore, the time for obtaining a polished surface with this quality is about 10 times less than the time required to polish a surface of brass of the same size.

3. Simple composite ferrule

Mechanical deformation is a change of geometry of the optical fibre away from a straight cylinder. Large-scale bending, or macrobending is where the radius of the curvature of the bend is very large in comparison to the core diameter. On the other hand microbends are deformations of the cylindrical core shape, which are small, compared to the fibre diameter (Ransey 1988). It is well known that mechanical deformation causes FRD by the formations of microbends in the fibre (Clayton 1989). When mounting the fibre, the appropriate epoxy and tubing should be selected, and general care must be taken to minimize mechanical stress and avoid additional FRD. Currently steel ferrules tubes are used to prepare the extremities of the optical fibres for general purposes, in test lab or even as a part of some instrument. Although it is clear that inefficiencies can result in the use of metal ferrules

submitted to low temperatures. Ferrules and inserts made with the composite described here, promises to be best option to handle the ends isolated of optical fibres.

3.1. Composite

While there is no direct evidence for the deterioration in Focal Ratio Degradation (FRD) of optical fibres in severe temperature gradients, the fibre ends inserted into metallic containment devices such as steel ferrules can be a source of stress, and hence increased FRD at low temperatures. In such conditions, instruments using optical fibres may suffer some increase in FRD and consequent loss of system throughput when they are working in environments with significant thermal gradients, a common characteristic of ground-based observatories. It is possible to use careful methodologies that give absolute measurements of FRD to quantify the advantages of using epoxy-based composites rather than metals as support structures for the fibre ends. This is shown to be especially important in minimizing thermally induced stresses in the fibre terminations. Furthermore, by impregnating the composites with small cerium oxide particles the composite materials supply their own fine polishing grit, Fig. 9, which aids significantly to the optical quality of the finished product. Different types of inserts are possible, Fig. 10, depending only on the precision of the machining.

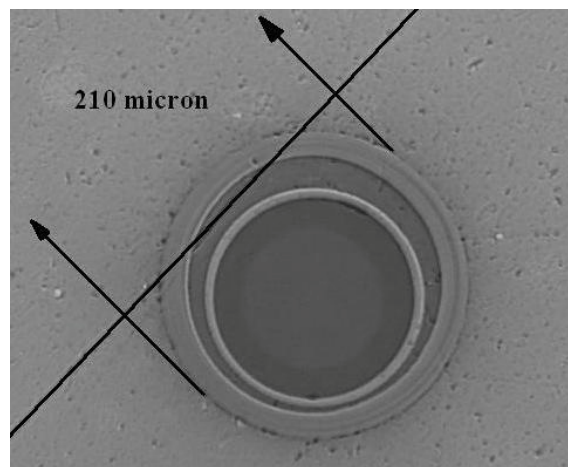


Figure 9. Microscopic photo of optical fibre inserted in a composite ferrule, after polishing procedure.



Figure 10. Inserts with optical fibres to be used in a fibres collector plate. Each insert can have several fibres.

4. Microholes arrays using plates of composite

A system like that shown in section 1, Fig. 2, presented a problem in the past: This problem was the terrific facility to detach the glass substrate of the metal brass polished. Variations of temperature at long of time cause different expansion in the metal brass and the glass. After some time, the UV epoxy normally used to glue the microlens arrays with the microholes array, cannot support more the bonding between the metal brass plates due to the successive expansions and contractions caused by temperature variations. Experiments using plates made with epoxy solidified, Fig. 11 can resolve this kind of problem in the range of temperatures between $-10\text{ }^{\circ}\text{C}$ and $22\text{ }^{\circ}\text{C}$, typical of high altitude, ground-based observatories. Although the coefficient of thermal expansion of epoxy, around 60×10^{-6} in/in/ $^{\circ}\text{C}$, is much greater than that of brass metal, steel metal or glass, its elasticity accommodates dimensional changes thermally induced. This means less pressure on the optical fibre and consequently avoids increases in FRD associated with stress but, in principle, could be deleterious in compromising the critical positioning of fibres as the temperature varies. The ideal condition requires a material with elasticity controlled so as not to cause stress or shift the positioning of optical fibre under temperature gradients.

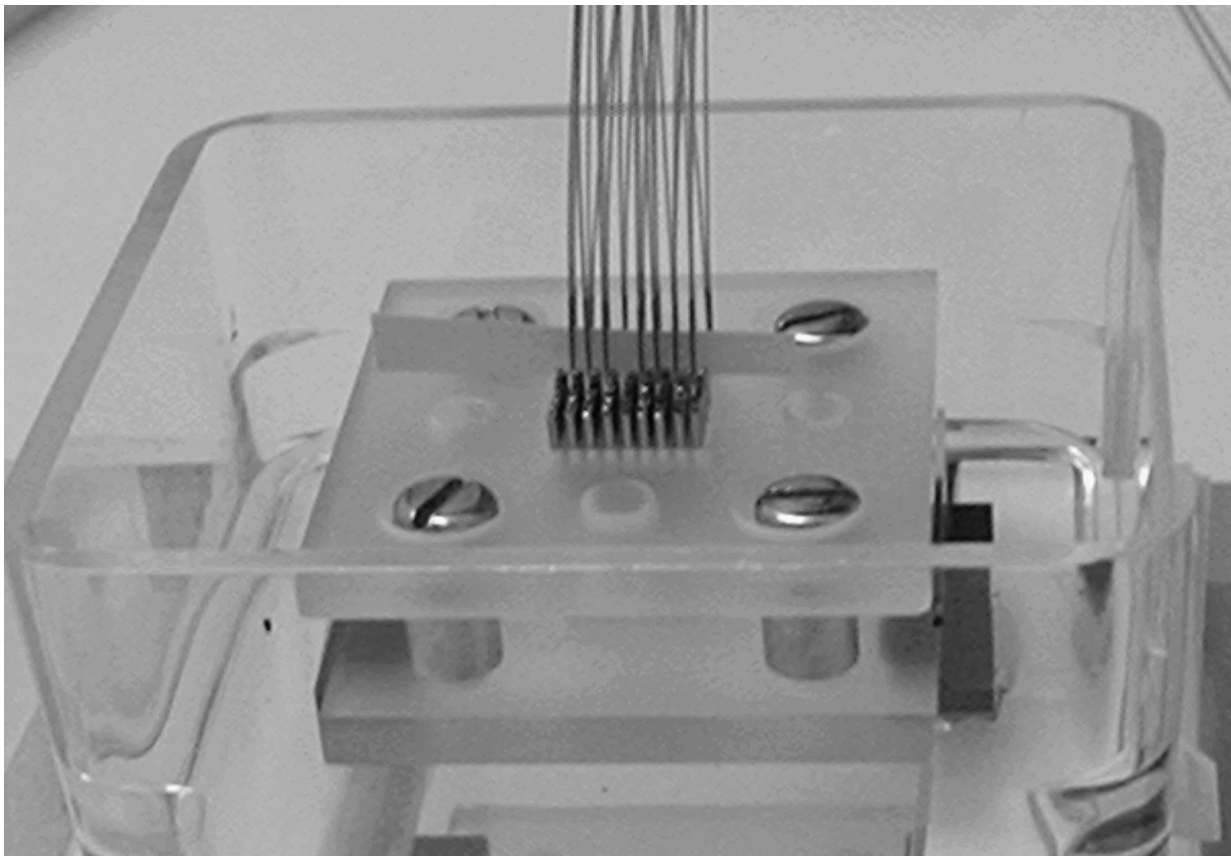


Figure 11. Microholes array device being prepared to be the input array of an IFU system

Notwithstanding the characteristics of this particular composite are still under study, this material was used successfully in the construction of devices for several fibres instruments. For example, we have used this composite to construct SIFS/IFU for the SOAR telescope in

Chile, (de Oliveira et al. 2010) and FRODOspec/IFU for the Liverpool Telescope, (Macanhan et al. 2006).

4.1. Construction of microholes arrays systems

To replace the brass metal or epoxy solidified and resolve the problems presented by both materials, we have used our composite to manufacture the parts of the microholes array device. The material composite obtained is less stressed and harder than EPOTEK 301-2 being a good choice to be used in optical fibres arrays. This material certainly has a combination of the characteristics from the epoxy and the refractory material oxides. The most important consequence of this combination is a coefficient of thermal expansion hither than metal brass but shorter than a simple epoxy solidified. The exactly number will depend of the relative concentration between the refractory material oxides and epoxy.

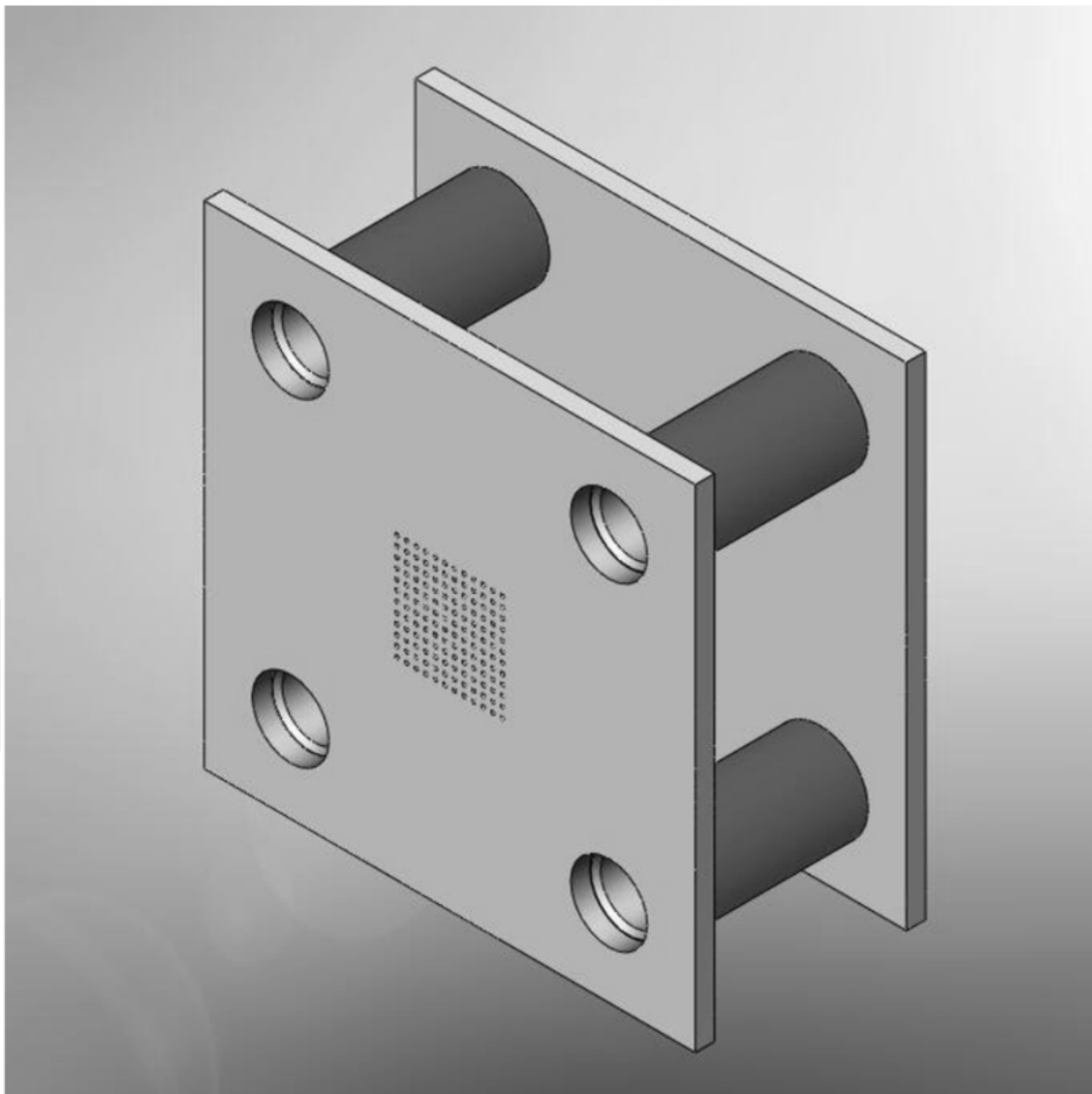


Figure 12. Schematic of the composite plates set to build the entrance device of lenslet IFU

In general, the schematic shown in Fig. 12 is the base of the entrance device of the lenslet IFU system. This device is much easier to be manufactured than the device described in section 1, Fig. 2. In fact, this new version does not require any precision in the holes confection on the composite plates. To obtain precision with the fibres position we have used a third plate called mask of precision, Fig. 13. This is a metal mask very thin obtained by a technique called electro formation. The mask obtained by this way may be configured to have holes with specific diameters and pits, with error around 1 micron in the diameter and in the position of the holes. This technique may produce a metal nickel plate with 200 microns of thickness and the procedure is very cheap. Taking in account these facilities; the mask will define the precision of the fibres array. It is possible to obtain micro holes with the diameter exactly one or two microns larger than the diameter of the fibre used. For another hand, the diameter of the holes in the composite plates does not need to have any precision and may be much larger than the diameter of the fibre. Since that, the step holes with different diameters in the composite plates it is not more necessary, also will be not necessary to use ferrules and any kind of protection to the fibres. Eventually a device like as shown in the Fig. 13 need to be made under a microscope because the diameter of the fibre may be much small and the number of fibres involved at the assemble may be high.

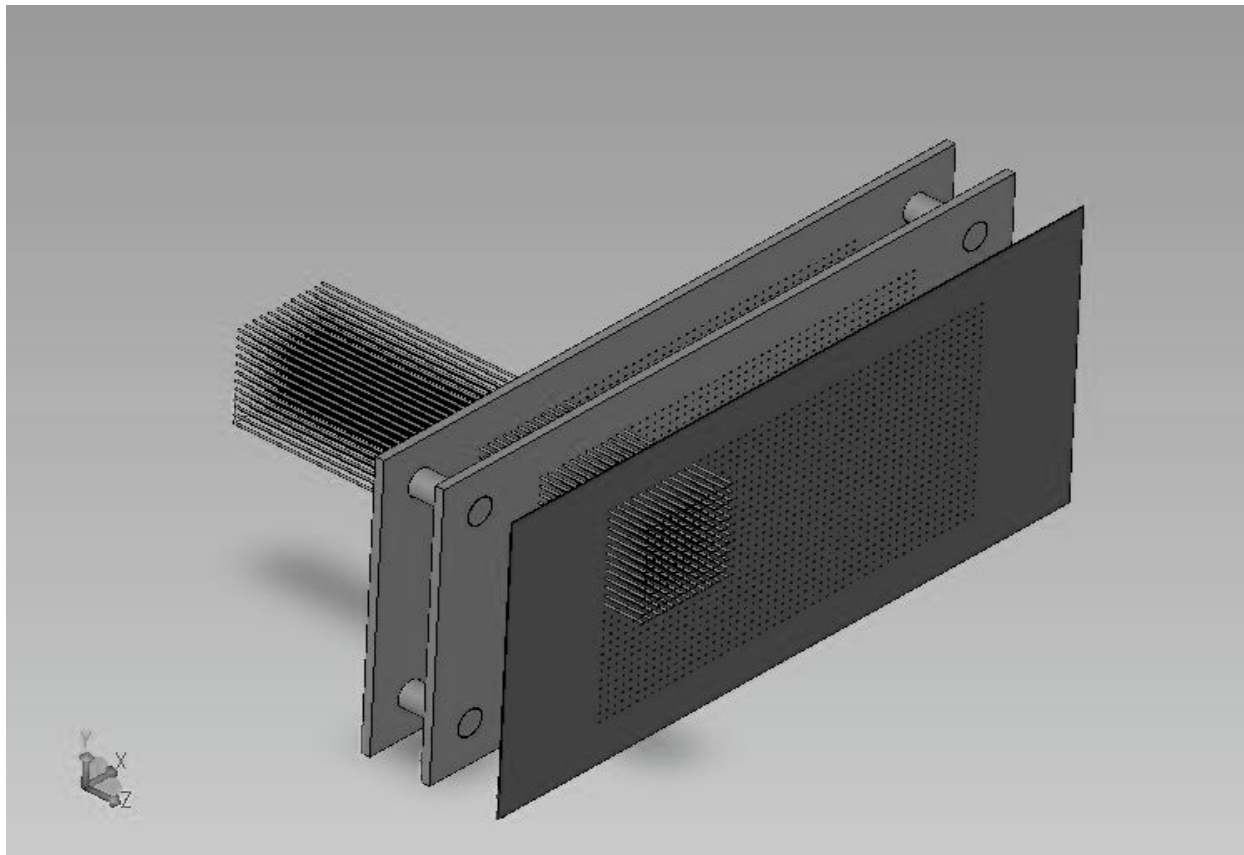


Figure 13. Entrance device during the assembling step, where the matrixes of holes in the composite plate set and in the precision mask are populated with the optical fibres terminations.

After assembled, the precision mask is glued against the composite plate and all set is immersed in EPOTEK 301-2 following the old procedure. To obtain the maximum throughput the surface of the fibres should be polished such that they are optically flat. This is the condition to attach the microlens array against the composite plate, Fig. 14 and Fig.15.

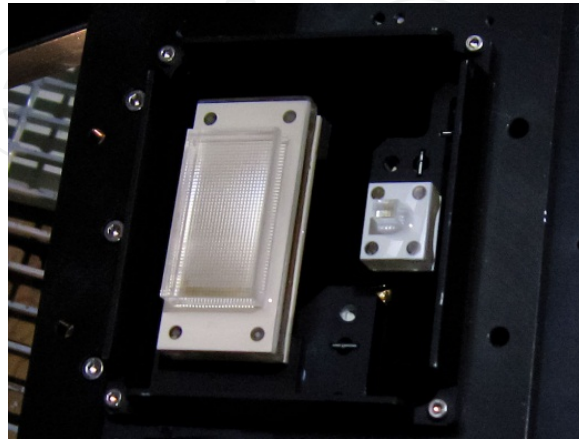


Figure 14. SIFS/IFU microlens glued

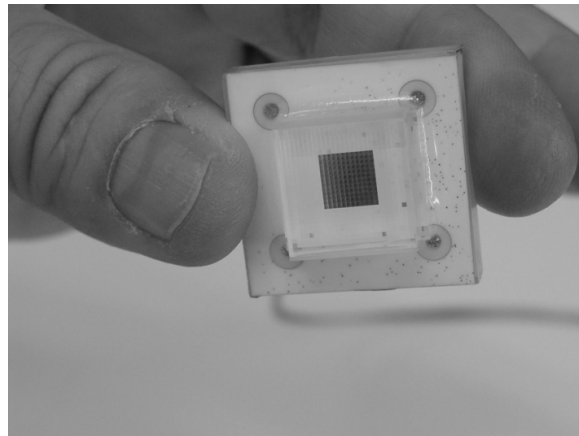


Figure 15. FRODOS IFU microlens glued

The pre-polishing process starts with the removal of excess glue with 2000 grit emery paper. Initial lapping with 6 μm diamond slurry on a copper plate and a second lapping with 1 μm diamond slurry on a tin-lead plate is used until the complete removal of the precision mask. Without the metal mask, the material of the composite plate is self-abrasive enough to produce a polishing of high performance of the optical fibres on a chemical cloth. This procedure is a basic condition to attach the microlens array against the composite plate of fibre terminations.

5. Characterization

The complete characterization of this composite may require several kinds of possible tests. However, applications with optical fibres in metrology involve analyses of displacement

when the device is submitted at thermal gradients. More specifically, optical fibres arrays used in astronomic instruments need to resist low temperatures without displacement of the fibre position and without delamination problem between parts. Simple experiments show that the linear CTE assumes values between 20 and $40 \times 10^{-6} / ^\circ\text{C}$ to $0 ^\circ\text{C}$ depending the concentration of the components. For example, a sample made with EPO-TEK 301-2, Barium oxide, Zircon oxide and Cerium oxide with proportions respectively 5:1:1:1, exhibits an α CTE around $30 \times 10^{-6} 1/^\circ\text{C}$.

Analysis of the Absolut Transmission in samples shows clearly that optical fibres inserted in brass or steel ferrules suffer increases in FRD when submitted to low temperatures. On the hand, the FRD increase in optical fibres inserted in ferrule made from EPO-TEK or in composite materials is minimised when submitted at the same negative variation of temperature. In fact, the result predicts a loss of around 10 per cent for the brass ferrules and around 3 per cent for the steel. Although it is clear that inefficiencies can result in the use of metal ferrules submitted to low temperatures, the losses are not easily quantifiable. The reason for this is that the ratio of the outer diameter of the fibre and the inside diameter of the ferrule defines the amount of epoxy between the ferrule and fibre. In the final analysis, this represents more or less compression in the fibre when the metal is compressed during the reduction of temperature.

5.1. Tests on fibres in an array

It is possible to do an experiment to observe the displacement of the fibres in an array of fibres constructed in the plates described in the section 4.2. An experimental array of 10×8 optical fibres is chosen as a representative test since it matches the base of the input array of IFUs as described before. A displacement is likely to occur with variations in temperature since the support material may suffer from some type of mechanical distortion. The experimental assembly consists of a support to hold the input array and to control thermal dissipation. A relay lens is used to project the image of the fibre array onto a CCD as a shown in the Fig. 16. The support to hold the array under examination (Fig. 17 and 18) is made of brass and had a canal for the introduction of liquid nitrogen. A continuous flux of dry nitrogen needs to be directed towards the surface of the input array to avoid condensation. Four small temperature sensors are cemented inside holes in the tested plate, close to the optical fibres. These sensors are necessary in order to test if the temperature along the plate reach thermalized state. A digital thermometer can be used to collect information from the sensors.

In our experiment, another sensor was installed inside the brass support together with a special electrical resistor to allow for temperature control. The temperature of the input array was controlled over a range between $23 ^\circ\text{C}$ and $-10 ^\circ\text{C}$. Images of the illuminated optical fibres can be obtained for a set of temperatures within the allocated range. With these images it is possible to obtain information regarding the change in the position of each fibre in the array. A simple algorithm may be used to process these results.

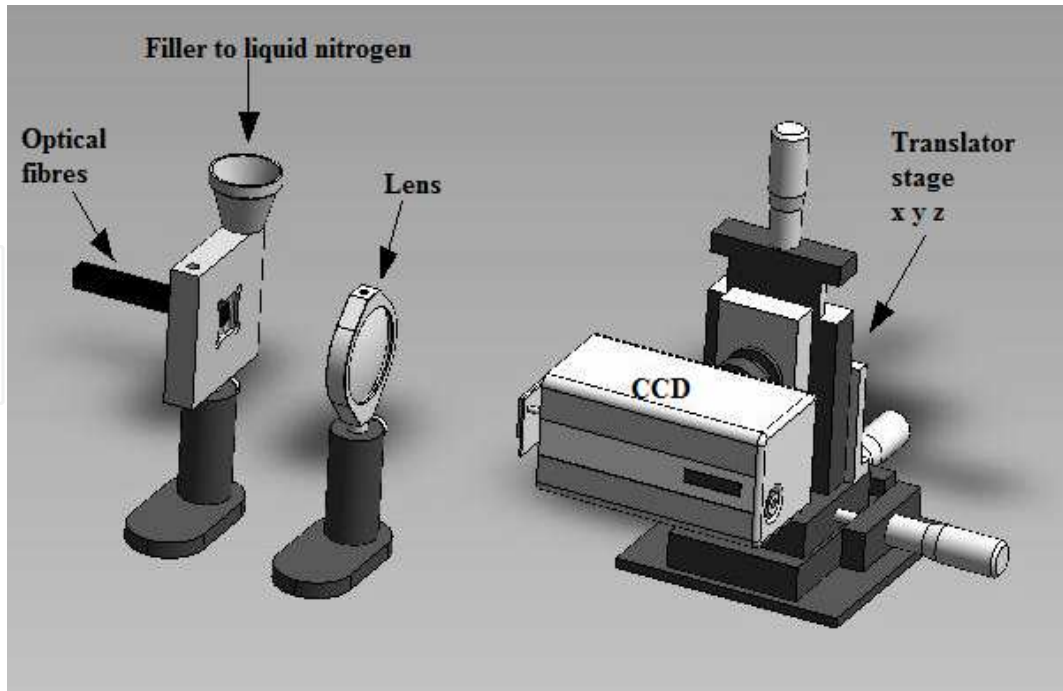


Figure 16. Diagram of the experimental set up to take images from the optical fibre array. The CCD is installed in a translation stage to put the image of the optical fibre illuminated exactly in the centre of the CCD plate. The holder support is used to keep the fibre plate array fixed and to control thermal dissipation.

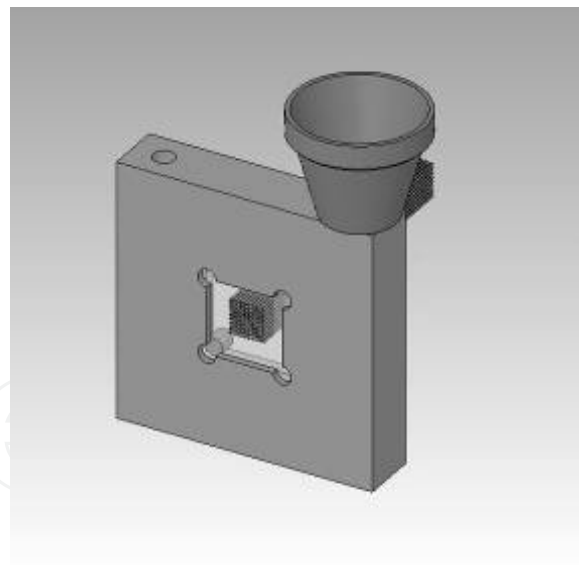


Figure 17. Schematic diagram of the holder where is fixed the fibre plate array.

5.2. Analyses of displacements of fibres in the array

An image analysis by software then determines the centroid of each bright spotlight projected by each fibre from the array on the CCD. Several images like the sample shown in the Fig. 19 are used to determine an average value in the position of each bright spot light. This associates position vectors connecting each bright spotlight with the origin. The first

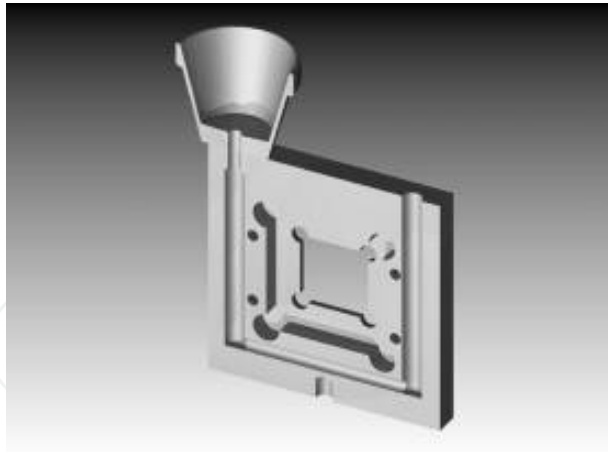


Figure 18. Schematic diagram of the holder showing the canal to flow the liquid nitrogen during the procedure to decrease the temperature. The holder is made of brass.

fibre at the top/left is used as a position reference. The variations of vector's modulus during the temperature gradient are computed to produce a graph with sub pixel precision (Neal et al. 1997). In this section we present results of tests using fibre arrays submitted to negative temperature gradients. The purpose of these tests is to analyse how much the fibres in the array may be displaced from their original position as a function of the expansion of the material during the change of temperature. Figs. 20, 21 and 22 show the behaviour of arrays with 80 optical fibres when submitted to four temperature gradients. The accuracy calculated for this experiment was less than $0.2\mu\text{m}$ and the continue curve represents a fitted function.

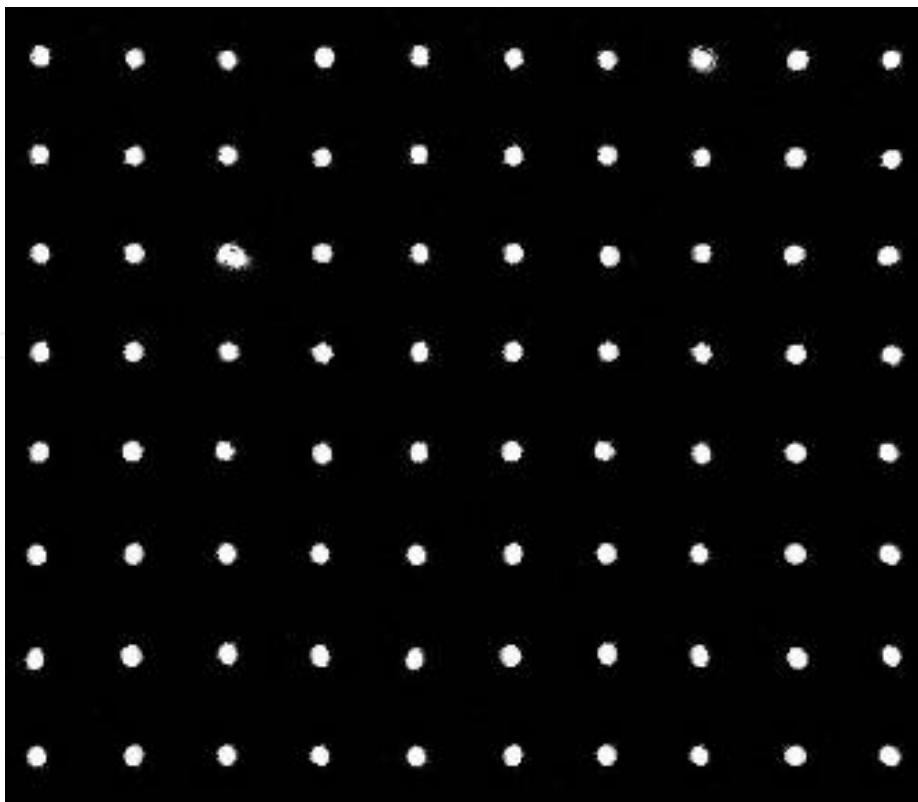


Figure 19. Image of the optical fibres matrix illuminated and projected on the CCD.

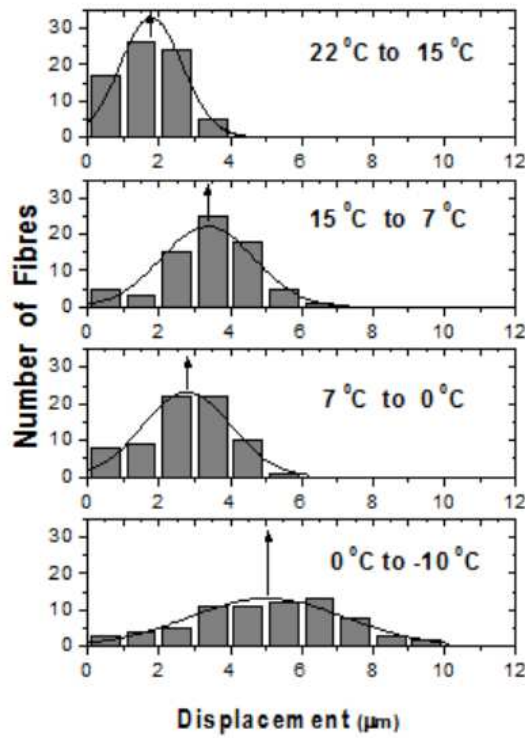


Figure 20. Distribution pattern of the optical fibres array constructed in metal brass plate submitted to four gradients of temperatures, 10 min each.

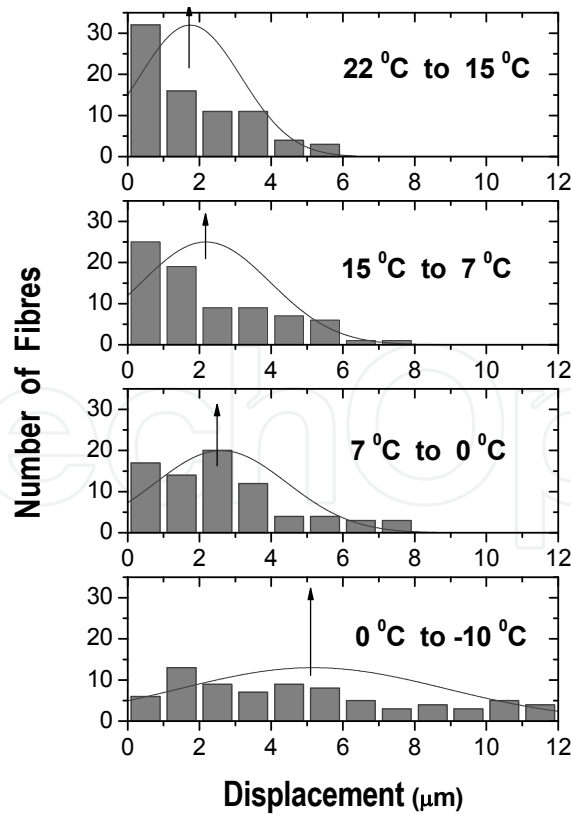


Figure 21. Distribution pattern of the optical fibres array constructed in epoxy EPO-TEK 301-2 submitted to four gradients of temperatures, 10 min each.

The bar graphs, demonstrates the distribution pattern of fibre positions as the temperature declines. It is possible to observe, the expansion of the EPO-TEK 301-2 epoxy material. The change in positions of the fibres amounts to $\sim 12\mu\text{m}$ as the temperature approaches -10°C . The array made of brass almost reaches this value despite having a totally different molecular structure to the epoxy. An interesting result was obtained with the optical fibre array in composite as may be observed in the Fig. 23. The behaviour of the composite array at low temperatures, represented in the bar graphs, is less noticeable than that obtained for the brass and epoxy arrays. In fact, when submitted to -10°C the change of the positions at the fibres is less than $6\mu\text{m}$. In the experimentation made with composite and brass plate samples, the temperature registered by all sensors on the plate was the same after some minutes and the error expected between the sensors would be around 0.2°C . However, we noted variations of $\sim 1.2^\circ\text{C}$ between the sensors in the experimentation with EPO-TEK plate. This may be explained by the fact that there are regions with different degrees of stress in the solidified EPO-TEK plate. These differences imply in a possible variation of thermal conductivity along the plate. As was shown in the section 2.3, stresses within solidified EPO-TEK 301-2 can be investigated with the use of the photo elasticity method whereby stress-induced birefringence is measured using polarised light. In fact it is quite common to observe static stress in plates of EPO-TEK solidified.

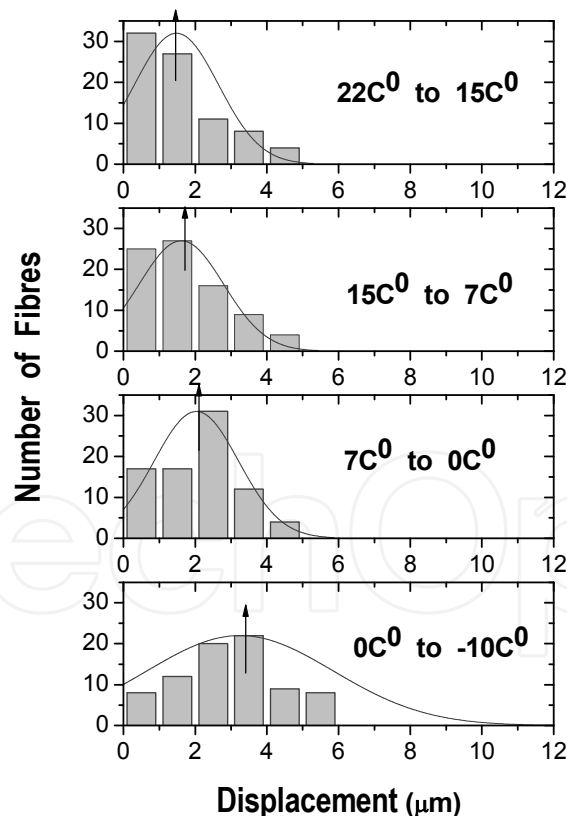


Figure 22. Distribution pattern of the fibres array in composite submitted to 4 gradients of temperatures, 10 min each.

The final conclusion for this experiment is that the composite epoxy material shows significant improvement and, in fact, has an even better performance than the brass or

epoxy solidified. The chosen composite material (EPO-TEK 301-2 + zirconium oxide) retains the beneficial bonding properties of the epoxy while avoiding its thermal displacement properties.

5.3. FRD in optical fibres samples

The mode dependent loss mechanisms are the causes of focal ratio degradation (FRD) in optical fibres, and are not often addressed by manufacturers. Mode dependent losses can be divided into two basic mechanisms. The first is waveguide scattering, which causes transfer of energy into loss modes by variations of the core diameter along the length of the fibre. The second is mechanical deformation. Mechanical deformation is a change of the geometry of the fibre away from a straight cylinder. Large scale bending, or macrobendings, is where the radius of curvature of the bend is very large in comparison to the core diameter. On the other hand, microbends are deformations of the cylindrical core shape, which are small, compared to the fibre diameter (Ransey 1988). It is well known that mechanical deformation causes FRD by the formation of microbends in the fibre (Clayton 1989). FRD is a non-conservation of *étendue* (or optical entropy) such that the focal ratio is broadened by propagation in the fibre. When mounting the fibre, the appropriate epoxy and, tubing should be selected and general care must be taken to minimise mechanical stress and avoid additional FRD.

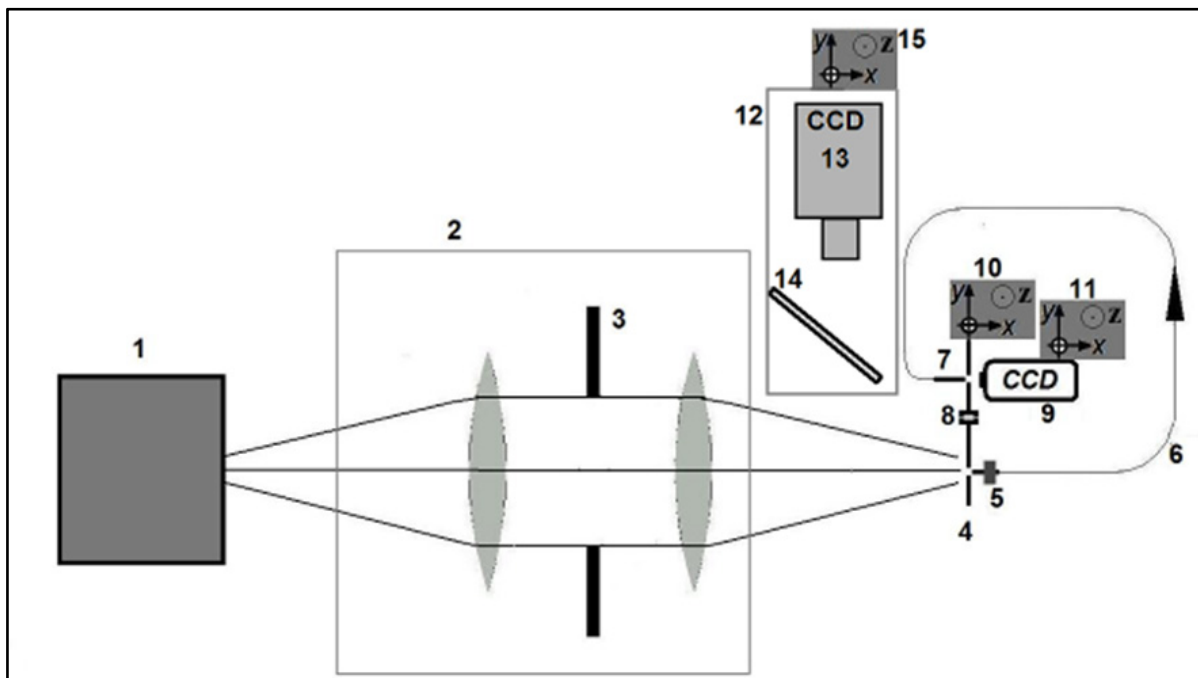


Figure 23. Diagram of the apparatus used to measure FRD – 1, light source, band pass filter and light diffuser; 2, telecentric optical system with unit magnification; 3, adjustable iris diaphragm; 4, alignment plate with a pinhole and both extremities of the tested fibre; 5, *peltier* device connected with the entrance of the optical fibre; 6, optical fibre; 7, exit of the optical fibre; 8, pinhole; 9, CCD; 10, xyz translation stage; 11, xyz translation stage; 12, microscope system; 13, CCD/lens; 14, beam splitter; 15, xyz translation stage

To measure the FRD properties of an optical fibre it is necessary to illuminate the test fibre with an input beam of known focal ratio. Then the output beam can be measured and compared with the input beam from a pinhole with the same diameter as the fibre core to determine the amount of FRD produced by the test fibre. The result is a plot of absolute transmission against output focal ratio. The experimental apparatus used to achieve this is illustrated in Fig. 23.

Illumination is provided by a 1-to-1 telecentric optical system that produces an image from an extensive uniformly illuminated source. This source is fed by a stabilized halogen lamp and has a band pass filter to provide light at 525nm, and filter's bandwidth of 100nm. An iris diaphragm placed in the collimated beam can be used to select the input focal ratio. A microscope with a CCD and beam splitter, monitored by a TV may be inserted between the pinhole/fibre plane, to be sure that the pinhole or the test fibre occupies the same position. To ensure accurate alignment of the fibre with the optical axis of the camera, the fibre is mounted in a tip-tilt translation stage. To begin the experiment, the pinhole device and the CCD are positioned to give us a reference image. In the test sequence, the pinhole is replaced with the entrance of the test fibre and the CCD is illuminated by the exit of the test fibre to give a projected image of the fibre. A distance of 9 mm between the CCD and the pinhole (or the entrance of the fibre in test) was determined as the best position to obtain images for optimal analysis. Background exposures are necessary for subtraction from the test exposures to remove the effects of hot pixels and stray light. In our experiments all fibres were tested at wavelength of 525nm, (defined using a Schott glass VG14 colour filter, ± 50 nm filter's bandwidth).

5.4. Reduction software

We have developed a custom software package (DEGFOC 3.0) to reduce the fibre images and to obtain throughput energy curves. This software works with PC microcomputers in a WINDOWS environment. We found this to be an effective solution for use in the optical laboratory environment allowing for ease of analysis. The DEGFOC 3.0 package gives curves of enclosed energy as is shown in the Fig. 24 with the option to save the result in ASCII format to be used in any graphic software, (eg: ORIGIN).

Fibre throughputs are automatically determined as a function of output focal ratio. The first step is an estimation of the background level to be subtracted from the test exposures to remove the effects of hot pixels and stray light. The software then finds the image centre by calculating the weighted average of all pixels. It associates a radius with each pixel and calculates the eccentricity that, in the ideal case, should be zero. Our target here is to obtain the absolute transmission of the fibre at a particular input f-ratio. After establishing the distance between the fibre test and the CCD, the software defines concentric annuli centred on the fibre image. These are then used to define the efficiency over a range of f-numbers at the exit of the fibre, where each f-number value contains the summation of all energy emergent from the fibre. Each energy value is calculated by the number of counts within each annulus divided by total number of counts from the pinhole images. The limiting focal

ratio that can propagate in the tested fibre is approximately $f/2.2$. Therefore we have defined $f/2$ to be the outer limit of the external annulus within which all of the light from the test fibre will be collected. The corresponding diameters of the annulus are converted to output focal ratios, multiplying them by the appropriate constant given by the distance between the fibre output end and the detector.

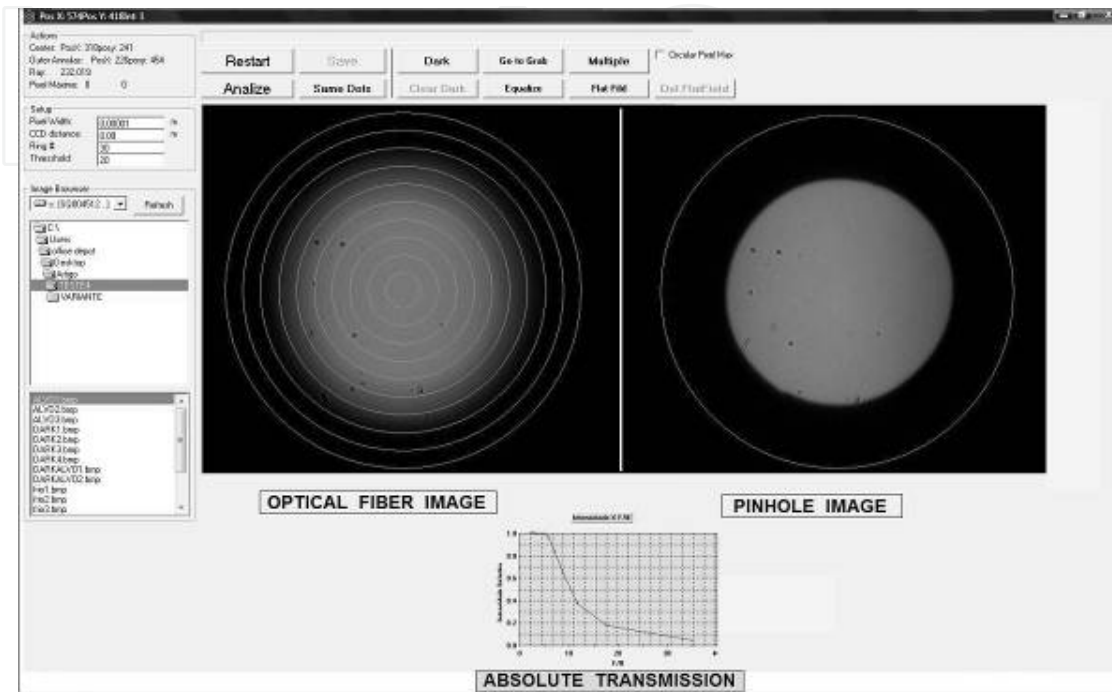


Figure 24. Print screen of the windows to the DEGFOC software.

5.5. Temperature gradient & FRD in optical fibres

In this experiment we have controlled the temperature of samples between $-10\text{ }^{\circ}\text{C}$ and $22\text{ }^{\circ}\text{C}$, typical of high altitude, ground-based observatories. To achieve this variation we have used a *Peltier* device coupled with a temperature sensor connected to an electronic controller. The end of the test fibre is placed in contact with the *Peltier* plate by a support, and to avoid problems with water condensation at low temperatures, the test ferrule is installed inside a plastic container with a glass window. A positive pressure of nitrogen gas is maintained using a flexible tube from a gas source. With these experimental arrangements it is possible to obtain images of the optical fibres with one of extremities inside a ferrule experiencing low temperatures without water condensation. This avoids the formation of ice at the end of the fibre that could attenuate the light at its termination and contaminate the results. Our aim is to measure the effect of constriction of the ferrule on the optical fibre caused by the gradient in temperature.

Plots of absolute transmission versus output focal ratio for three samples in four configurations are presented here. We have plotted graphs with the extremes curves obtained at room temperature of $23\text{ }^{\circ}\text{C}$ and at $-10\text{ }^{\circ}\text{C}$ after a time interval of 30 min. chosen to stabilize the thermal effects between one measurement and next. The throughput graph

obtained from one fibre with brass ferrule, in dry atmosphere, is shown in Fig. 25. These results show an increase in FRD when the brass ferrule experiences a cold temperature. The total variation observed in the hatched area is very strong and diminishes as the output focal ratio of the fibre is increased. An analysis of the results demonstrates that the loss of light at F/2.3 would be around 10 per cent. This degradation is caused, presumably, by the contraction of the brass ferrule with decreasing temperature causing compressive stress of the ferrule on the fibre. The error bars, of ± 1 per cent, together the average curves, were defined after repeating each experimentation at least six times. Some experimental uncertainty in the control of temperature causing small variations in the compression force on the ferrule/fibre and consequently cause small variations in the throughput of the sample. However is evident the presence of some dissipative process, which changes the borderline of the stress during the variations of temperature. Taking in account that the experiment is made with input focal ratio around the Numerical Aperture of the fibre (F/2.27) there is the possibility that it is changing because the stress.

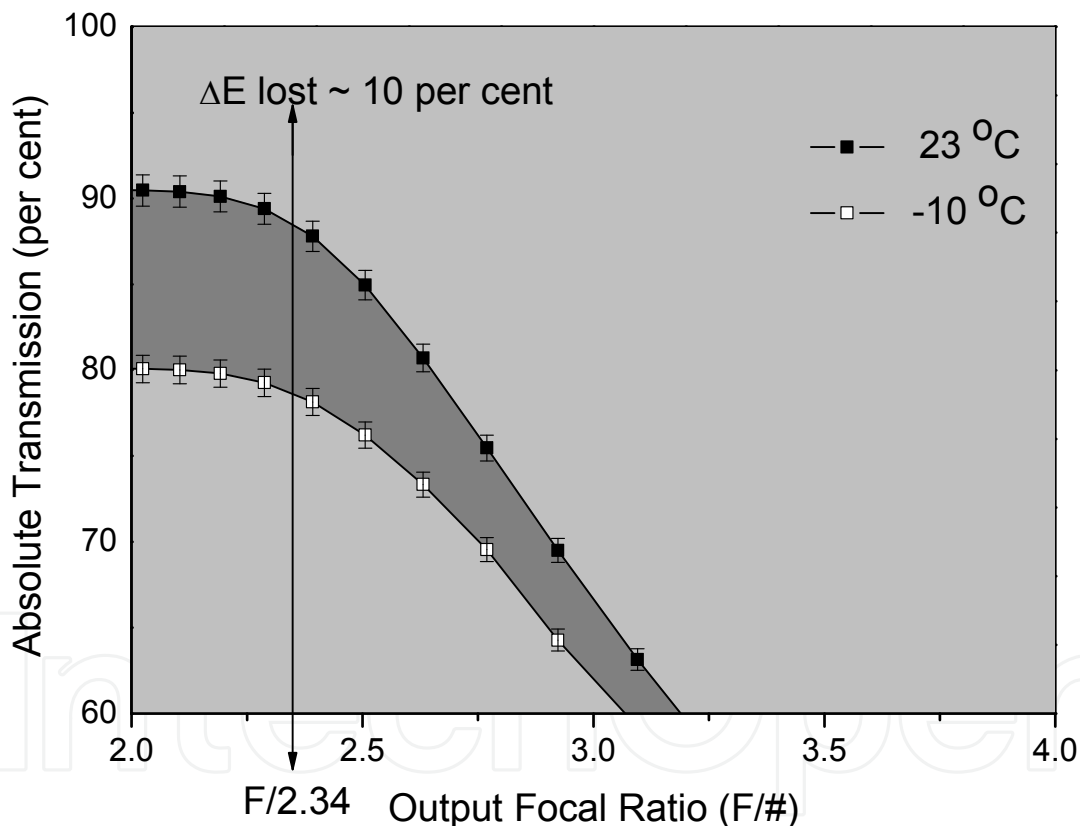


Figure 25. Performance of the optical fibre using brass ferrule. The ferrule was submitted to a negative temperature gradient of 23 °C in a dry atmosphere. The gradient was obtained, reducing the temperature, 23 °C to -10 °C, in 30 min of interval time. Two extremes curves were measured in this interval, producing the hatched area.

Such effects are critical to the design and implementation of fibre spectrographs. These results imply serious restrictions in the use of metal ferrules for optical fibres operating in ambient conditions that experience large changes of temperature typical of many observatories both during the night and throughout the year.

The throughput for samples with fibres inserted into epoxy ferrules and composite ferrules, in dry atmosphere, are shown for comparison in Figs. 26 and 27 using the same experimental procedures. Both graphs, present a very similar curves, with loss of light at F/2.34 around 2 per cent to the epoxy ferrule and 1 per cent to the composite ferrule. It seems that the loss of energy through stress-induced FRD effects is significantly less than that observed with the metal ferrule samples. The similarity of the epoxy and composite results imply that we are seeing similar effects due to the similar structure of both materials. In fact the composite material uses the same epoxy as a substrate. A natural compression happens during the cooling process, but does not produce a compressive stress of the brass ferrule on the fibre. The elastic properties of the epoxy may neutralize the mechanical stress on the fibre during the contraction process. The same error bars, of ± 1 per cent, were obtained after six repetitions of the experiment.

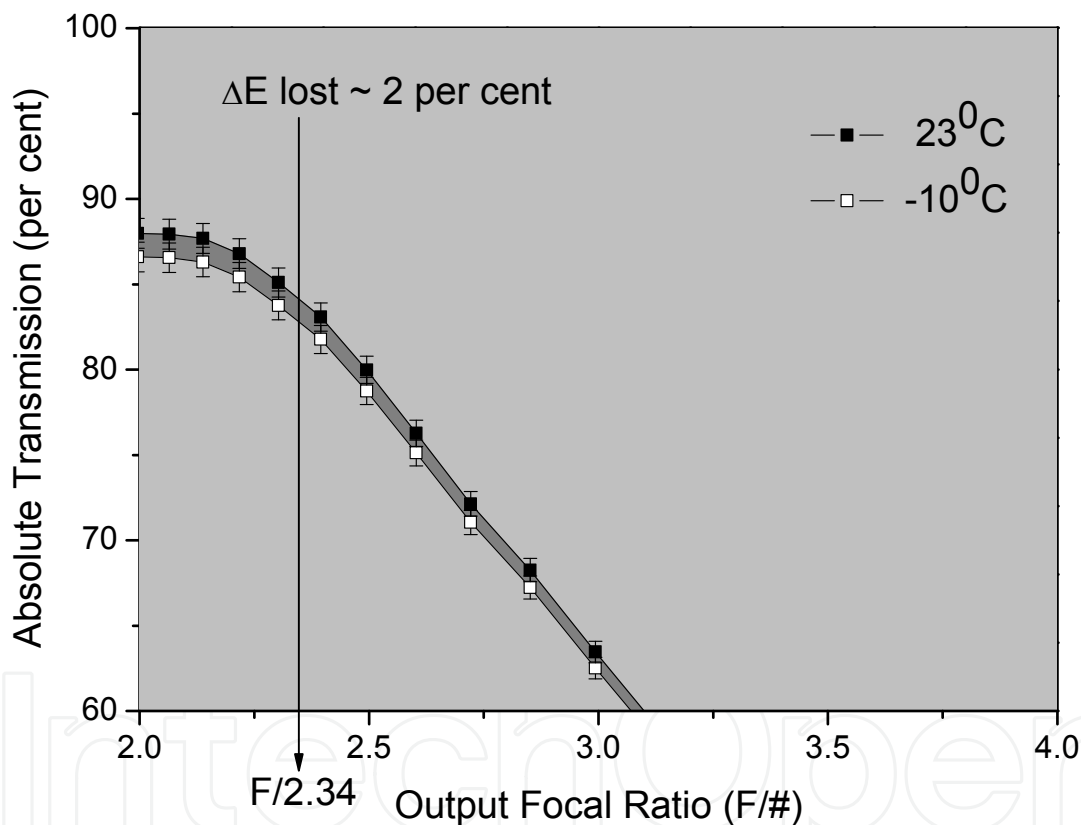


Figure 26. Performance of the optical fibre using epoxy ferrule. The ferrule was submitted to the negative temperature gradient following the same conditions of the experimentation using metal ferrule.

In general, the variation in the FRD results obtained with different samples from the same optical fibres is ± 1 per cent because the noise of the measurements. Analyse of the throughput curves obtained at room temperature from the epoxy and composite ferrules is ~ 3 per cent less on average when comparing the same curve obtained from the metal ferrules samples. The explanation for this difference may be in the aging process of the epoxy and composite ferrules. Both samples were submitted to six thermal cycles, between 50 °C and -

20 °C after machining to avoid anomalous results during the experimentations. However, this procedure may increase the intrinsic FRD of the fibre given that the material structure of the ferrule may suffer accommodation pressing the fibre extremity. On the other hand, small differences of size in the hatched area of lost energy between similar samples could be expected. Differences like that would be explained by the difficulty to quantify the total length of the fibre immersed in epoxy inside the ferrule. The procedure of inserting fibre and epoxy into the ferrule is virtually handmade. There is no way to accurately control the amount of epoxy into opaque ferrules, because it is not possible to visualize the level of epoxy. Exception perhaps for polished quartz ferrules. Obviously, the length of fibre immersed in epoxy defines the length that would be submitted at the stress from the ferrule contraction.

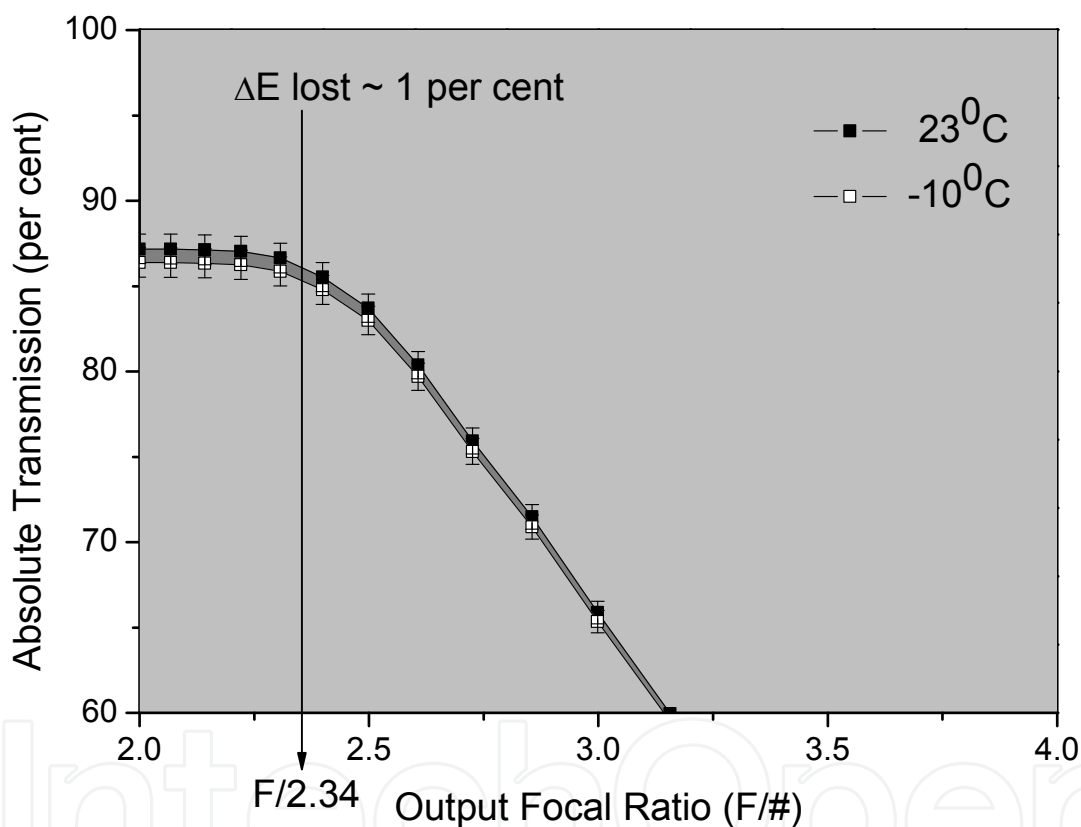


Figure 27. Performance of the optical fibre using composite ferrule. The ferrule was submitted to the same negative temperature gradient of the anterior experimentation using metal ferrule, steel ferrule and epoxy ferrule.

6. Polishing substrate

There are two ways of surface preparations in optical fibres, cleaving and polishing. In general applications directed to scientific instrumentation require optical fibres with extremities polished. This is the way where it is possible to optimize the spot light from the optical fibre. Furthermore, all fibre connectors require polishing and high performance may be reached with special machines and dedicated procedures. Currently, polishing procedures

to optical fibres are based on very delicate glass paper or lapping discs soaked in abrasive liquid solutions. Often, this kind of liquid abrasive is very expensive taking in account your composition based in sophisticated chemistry keeping micro diamonds in suspension. Other options, considers abrasive silica and aluminium oxide mixed with oil solution or water solution. A very interesting application for the composite described here is its use as a high-performance abrasive disc to polish optical fibres.

6.1. Abrasive discs of composite to polish optical fibres

It is possible to fabricate composite discs, controlling the abrasive capacity through the correct choice of oxide and quantity mixed with epoxy. There are several manufacturers of oxide refractory with high purity such that it is possible to compose a complete grid of polishing discs. We can consider two major advantages in the use of polishing discs manufactured with composite: The first lies in the fact that the entire polishing process can be done using distilled water only. The second advantage is that after the polishing procedure, the disc can be restored to its original flatness and completely cleaned by machining process. The efficiency of this composite disc to polish optical fibres is based in the fact that some of the oxides of the mixture are naturally abrasives. Materials like cerium oxide or silica oxide can be prepared in liquid solutions abrasives and has been used for a long time in polishing procedures of lenses and other optical devices. Discs of composite can be made in any size and can easily be adapted in the rotation device of polishing machine. Fig. 28 shows an array of optical fibres polished using discs of composite.

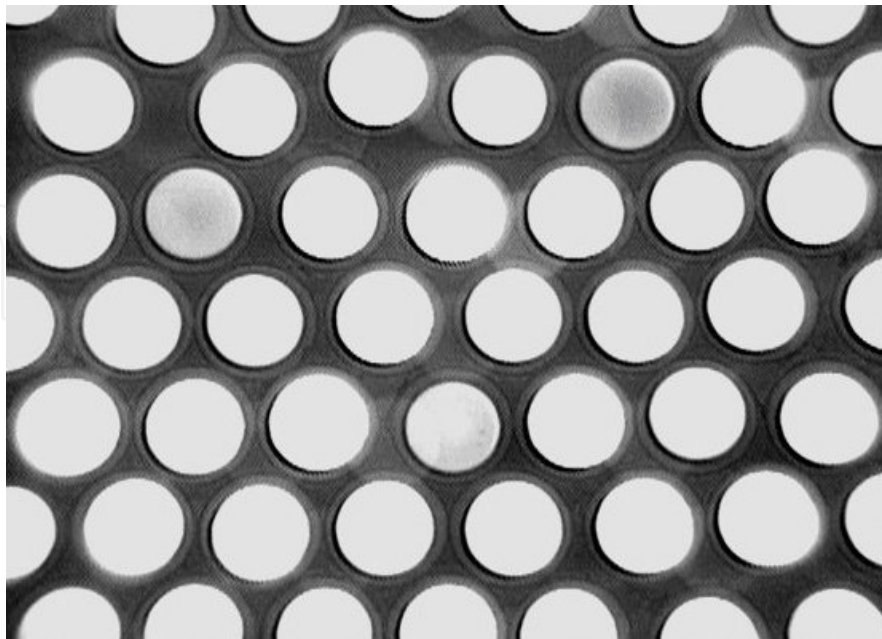


Figure 28. Microscopic photo of part of the optical fibres array, after polishing procedure, using discs of composite containing cerium oxide.

7. Conclusion

The motivation of this work was to test the performance of optical fibres inserted in ferrules made with different materials at low temperatures. The problem of finding a material best suited to securing fibres for astronomical spectrographs to cope with thermal stresses, FRD minimization and the need to achieve adequate polishing finish led us to investigate the use of composite materials. As has already been demonstrated, epoxies can be used not only as a means of holding fibres within structures (slit blocks, fibre arrays etc.) but also as a material to fabricate the structures themselves. The properties that require investigation in this context are CTE matching, machinability, bonding to glass and ease of polishing. In this context we have made several samples to evaluate FRD performance and position displacement of the inserted fibres when submitted to low temperatures.

Author details

Antonio C. de Oliveira and Ligia S. de Oliveira

Laboratório Nacional de Astrofísica / Ministério da Ciência Tecnologia e Inovação, Brazil

Acknowledgement

This work was financially supported by the FAPESP project no. 1999/03744-1 and CNPq project 62.0053/01-1- PADCT III/ Milenio. We wish to thank the staff of the Laboratório Nacional de Astrofísica/ MCT.

8. References

- Clayton, C. A. (1989). The Implications of Image Scrambling and Focal Ratio Degradation in Fibre Optics on the Design of Astronomical Instrumentation, *Astronomy and Astrophysics*, Vol. 213, No. 1-2, (April 1989), pp. 502-515, ISSN 0004-6361
- de Oliveira, A. C. et al. (2002). The Eucalyptus Spectrograph, *Proceedings of SPIE Instrument Design and Performance for Optical/Infrared Ground-based Telescopes*, pp. 1417-1428, Waikoloa, Hawaii, USA, August 25-28, 2002
- de Oliveira, A. C. et al. (2005). Studying Focal Ratio Degradation of Optical Fibres with a Core Size of 50 μm for Astronomy, *Mon. Not. R. Astron. Soc.*, Vol. 356, No. 3, (October 2004), pp. 1079-1087, ISSN 00358711
- de Oliveira, A. C. et al. (2010). The SOAR Integral Field Unit Spectrograph Optical Design and IFU Implementation, *Proceedings of SPIE Modern Technologies in Space- and Ground-based Telescopes and Instrumentation*, pp. 77394S-1-77394S-12, San Diego, California, USA, June 27, 2010
- Ransay, L. W. (1988). Focal Ratio Degradation in Optical Fibers of Astronomical Interest, In: *Fiber Optics in Astronomy*, Samuel C. Barden, pp. 26-40, Astronomical Society of the Pacific, ISBN 0-937707-20-1, San Francisco, California, USA

Macanhan, V. B. P. et al. (2006). FRODOSPEC Integral Fibre Unit, Proceedings of SAB XXXII Reunião da Sociedade Astronômica Brasileira, pp. 194-195, Atibaia, São Paulo, Brasil, August 3, 2006

IntechOpen

IntechOpen